

## Dynamics of protein hydration water

M. Wolf, S. Emmert, Rudolf Gulich, Peter Lunkenheimer, Alois Loidl

### Angaben zur Veröffentlichung / Publication details:

Wolf, M., S. Emmert, Rudolf Gulich, Peter Lunkenheimer, and Alois Loidl. 2015.  
"Dynamics of protein hydration water." *Physical Review E* 92 (3): 032727.  
<https://doi.org/10.1103/physreve.92.032727>.

### Nutzungsbedingungen / Terms of use:

licgercopyright

Dieses Dokument wird unter folgenden Bedingungen zur Verfügung gestellt: / This document is made available under these conditions:

**Deutsches Urheberrecht**

Weitere Informationen finden Sie unter: / For more information see:

<https://www.uni-augsburg.de/de/organisation/bibliothek/publizieren-zitieren-archivieren/publiz/>



## Dynamics of protein hydration water

M. Wolf, S. Emmert, R. Gulich, P. Lunkenheimer,<sup>\*</sup> and A. Loidl  
*Experimental Physics V, Center for Electronic Correlations and Magnetism,  
 University of Augsburg, Universitätsstr. 2, 86135 Augsburg, Germany*

(Received 29 November 2014; revised manuscript received 17 August 2015; published 28 September 2015)

We present the frequency- and temperature-dependent dielectric properties of lysozyme solutions in a broad concentration regime, measured at subzero temperatures, and compare the results with measurements above the freezing point of water and on hydrated lysozyme powder. Our experiments allow examining the dynamics of unfreezable hydration water in a broad temperature range. The obtained results prove the bimodality of the hydration shell dynamics. In addition, we find indications of a fragile-to-strong transition of hydration water.

DOI: [10.1103/PhysRevE.92.032727](https://doi.org/10.1103/PhysRevE.92.032727)

PACS number(s): 87.15.kr, 77.22.Gm, 87.14.E-, 87.15.H-

### I. INTRODUCTION

Water is essential for nearly all biologically active systems. Prominent examples are globular proteins, whose functional and physical properties are fundamentally determined by the presence of water [1,2]. Especially, the so-called hydration water, i.e., the shell of water molecules in the close vicinity of the protein surface, strongly interacts with the latter. As a consequence, hydration water does not crystallize, even at temperatures far below water's nominal freezing point. Due to their importance, protein-solvent interactions are a very active field of research [1,3–8]. It is commonly believed that the water molecules of the hydration shell cause a relaxation process similar to that of pure water but slowed down due to the bonding to the protein. However, it is a matter of debate if there are *two* such hydration-shell relaxations [9–14], which would be in accordance with the idea that there are at least two layers of hydration water with different bonding energies. This is difficult to decide because proteins exhibit numerous intramolecular motions and solvent interactions, all giving rise to relaxation processes complicating the dielectric spectra of protein solutions.

Figure 1(a) schematically shows the contributions of the major relaxation processes of protein solutions to dielectric loss spectra,  $\varepsilon''(\nu)$ . Here one should be aware that most of them only show up after subtraction of strong ionic conductivity and electrode-polarization (EP) effects (grey region), typical for ion-conducting materials [16–21]. Protein solutions always show one or two so-called  $\beta$  relaxations, resulting from the tumbling of the dipolar protein, and a very strong  $\gamma$  relaxation caused by the dipolar water molecules [11,12,14,22–26]. To avoid confusion, here some remarks on nomenclature seem appropriate as the denotation of different dynamical processes is rather ambiguous in literature. For example, in contrast to the above definition, following the biophysical notation, in the field of supercooled liquids the term “ $\beta$  relaxation” denotes a universal secondary process that is faster than the structural  $\alpha$  relaxation [27–29]. The mentioned  $\gamma$  relaxation would correspond to the  $\alpha$  relaxation of bulk water in this nomenclature. Moreover, it was proposed that the dynamics of water in solutions, in confinement, and in biological interfaces exhibits

a universal low-temperature process with Arrhenius temperature dependence that also was termed  $\beta$  relaxation [30]. In the present work, however, we label the different processes according to the biophysical nomenclature, where  $\beta$  relaxation denotes the tumbling of dipolar biological molecules in solution, and the motion of free water molecules is termed  $\gamma$  relaxation. In addition to these processes, protein solutions may also exhibit proton-fluctuation processes (in the frequency range of the  $\beta$  relaxation) [31] or sub- $\beta$  relaxations, caused by conformational sampling events [32]. The hydration-shell relaxations are expected to be located in the so-called  $\delta$ -dispersion region between the  $\beta$  and  $\gamma$  relaxations. As pointed out earlier [14], a single relaxation function sufficiently describes the  $\delta$ -dispersion region of protein solutions and, according to Occam's razor, there is no reason to employ a further relaxation function to account for the experimental data. On the other hand, a proper analysis of the  $\delta$  dispersion is difficult because large parts of the relevant frequency region are dominated by the  $\beta$  and  $\gamma$  relaxations [Fig. 1(a)]. In addition, other contributions such as protein side-chain motions or internal protein motions may also contribute in this frequency range [12,24,33–35]. An often used alternative approach is the investigation of hydrated protein powders [3,36–38]. However, their dynamics also reveals numerous relaxations, with some of them being extremely hydration dependent [39–43]. Thus, the interpretation of hydrated protein-powder studies is difficult, too.

The approach of the present work is to circumvent these problems by investigating protein solutions *below* the freezing point of water. In this way, the interfering  $\beta$  and  $\gamma$  relaxations are eliminated since the protein and water molecules cannot easily reorient in the frozen sample and also the conductivity is strongly reduced. In contrast, as the hydration-shell water remains amorphous, the  $\delta$  relaxation(s) should still be observable. The typical  $\varepsilon''$  spectrum of a frozen protein solution is shown in Fig. 1(b). The strong relaxationlike processes at low frequencies (EP1, EP2) arise from dc conductivity and nonintrinsic EP effects. The relaxation termed “ice” is caused by Bjerrum and ionic defects in the ice structure resulting in proton-hopping processes, physically equivalent to reorientations of water molecules [44,45]. In the  $\delta$ -dispersion region, two  $\delta$  relaxation processes are indicated ( $\delta_1$ ,  $\delta_2$ ).

In the present study, we investigate various frozen lysozyme solutions and compare the results with those of protein solutions above the freezing point [14] and with a hydrated lysozyme powder. This gives valuable insight into the

<sup>\*</sup>Corresponding author: peter.lunkenheimer@physik.uni-augsburg.de

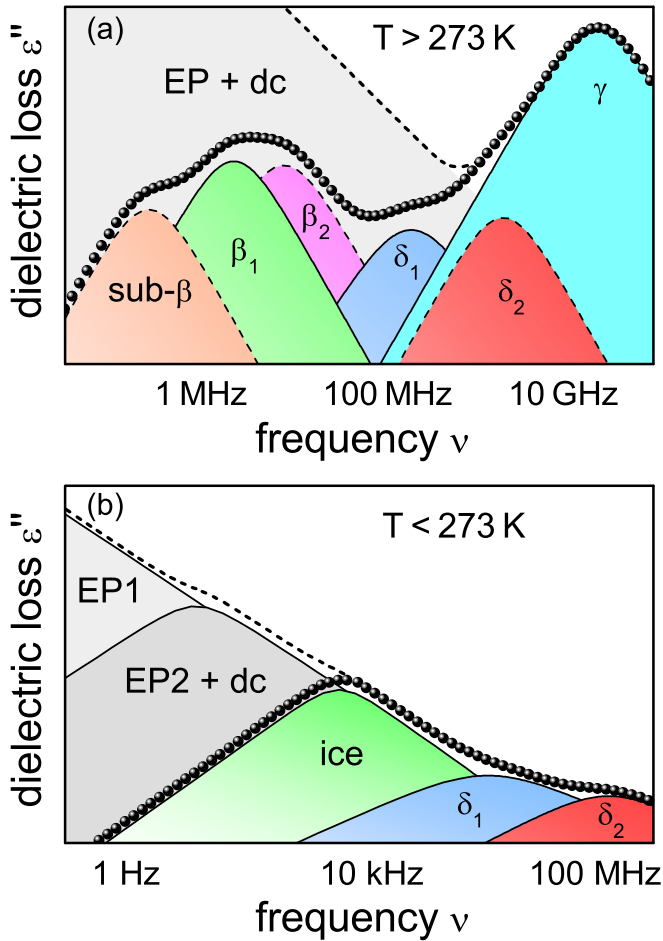


FIG. 1. (Color online) Schematic plot of the dielectric loss of protein solutions above (a) and below (b) the freezing point of water (the labeling of the different processes follows the biophysical nomenclature). The circles show the loss after subtraction of the dc conductivity and EP contributions (grey regions). Frame (a) comprises the major processes hitherto found in protein solutions [15]: The commonly observed  $\beta$  and  $\gamma$  relaxations are due to the reorientational motions of the dipolar protein and water molecules, respectively. The  $\delta$  relaxations are ascribed to hydration water. Additional contributions may arise from conformational sampling (sub- $\beta$ ). (b) Frozen lysozyme solutions show three intrinsic relaxations: The “ice” process results from proton hopping in the ice matrix. In the frequency range of the  $\delta$  dispersion, two relaxations are depicted ( $\delta_1$ ,  $\delta_2$ ).

hydration-shell dynamics of proteins in a broad temperature range and helps clarify the question of whether there are indeed two  $\delta$  relaxations. Moreover, we find indications for a crossover in the temperature dependence of the relaxation time of loosely bound hydration water from so-called fragile temperature characteristics described by the Vogel-Fulcher-Tammann (VFT) law to a weaker temperature dependence, following Arrhenius behavior.

## II. EXPERIMENTAL DETAILS

The complex dielectric permittivity and conductivity were determined using two measurement devices covering the

frequency range between  $\approx 0.1$  Hz and 3 GHz [46,47]. For the low-frequency range (0.1 Hz–10 MHz) a Novocontrol Alpha-A Analyzer was employed. This frequency-response analyzer enables high-precision measurements by directly measuring the sample voltage and the sample current by means of a lock-in technique. The sample is kept in a parallel-plate capacitor made of platinum (diameter 4.8 mm, plate distances  $d = 0.1$ –0.85 mm), which is mounted into a  $N_2$ -gas cryostat (Novocontrol Quatro) allowing temperature-dependent measurements. In the frequency range 1 MHz–3 GHz, a coaxial reflection method was used employing the Agilent Impedance/Material Analyzer E4991A. Here, the sample capacitor is connected to the end of a coaxial line, thereby bridging inner and outer conductors. To eliminate contributions of coaxial line and connectors, a calibration with three standard impedances is necessary. Temperature-dependent measurements are enabled by placing the capacitor in a  $N_2$ -gas cryostat (Novocontrol Quatro). The connection between the sample and the measurement device within the cryostat is established by a specially designed sample holder [46].

Dialyzed and lyophilized hen egg white lysozyme powder ( $M = 14.3$  kDa) was purchased from Sigma-Aldrich (Fluka 62970) and used without further purification. Lysozyme-water solutions (mixtures) were prepared by dissolving weighed amounts of protein powder in deionized  $H_2O$  (Merck “Ultrapur”). In this way, protein solutions with concentrations between 3 and 100 mmol of protein per liter of water were prepared (corresponding to 42.9–1430 mg of protein per ml of water, room temperature). The pH values of these solutions are in the range 2.8–3.8 (measured with a pH tester from Hanna-Instruments). The hydrated lysozyme powder was prepared by exposing the powder of the same type as above (Fluka 62970) to an atmosphere with a defined relative humidity of 97–98% ( $T = 25$  °C), ensured by a saturated  $K_2SO_4$  solution in an exsiccator. The degree of hydration was determined to be  $h = 30$  wt%, i.e., 0.3 g of water per gram of sample.

## III. RESULTS AND DISCUSSION

Figure 2(a) shows broadband spectra of the dielectric constant of a 10 mmol/l lysozyme solution measured at different temperatures *below* the freezing point of water [for  $\varepsilon''(\nu)$  see Appendix A]. Starting at a low-frequency value of  $10^7$ ,  $\varepsilon'(\nu)$  at 260 K drops to a value of the order of 10 at  $\nu \approx 5$  MHz in three consecutive steps, indicating the existence of three relaxation processes (EP1, EP2, and ice). Based on the unreasonably high dielectric strengths, relaxations EP1 ( $\Delta\varepsilon > 10^6$ ) and EP2 ( $\Delta\varepsilon > 10^3$ ) are attributed to EP effects often found in ionically conducting materials [16–21]. In contrast, the third  $\varepsilon'(\nu)$  step with  $\Delta\varepsilon$  of the order of 100 is due to the typical relaxation process of ice arising from the mentioned proton-hopping processes [44,48,49]. With decreasing temperature, all these relaxation features shift to lower frequencies, directly mirroring the decreasing translational mobility of free ions and protons. At frequencies higher than 500 kHz, two additional relaxations are found. Hardly detectable in the scaling of Fig. 2(a), they become evident in the enlarged views of Figs. 2(b) and 2(c) showing  $\varepsilon'$  and  $\varepsilon''$  in the high-frequency range. These figures provide

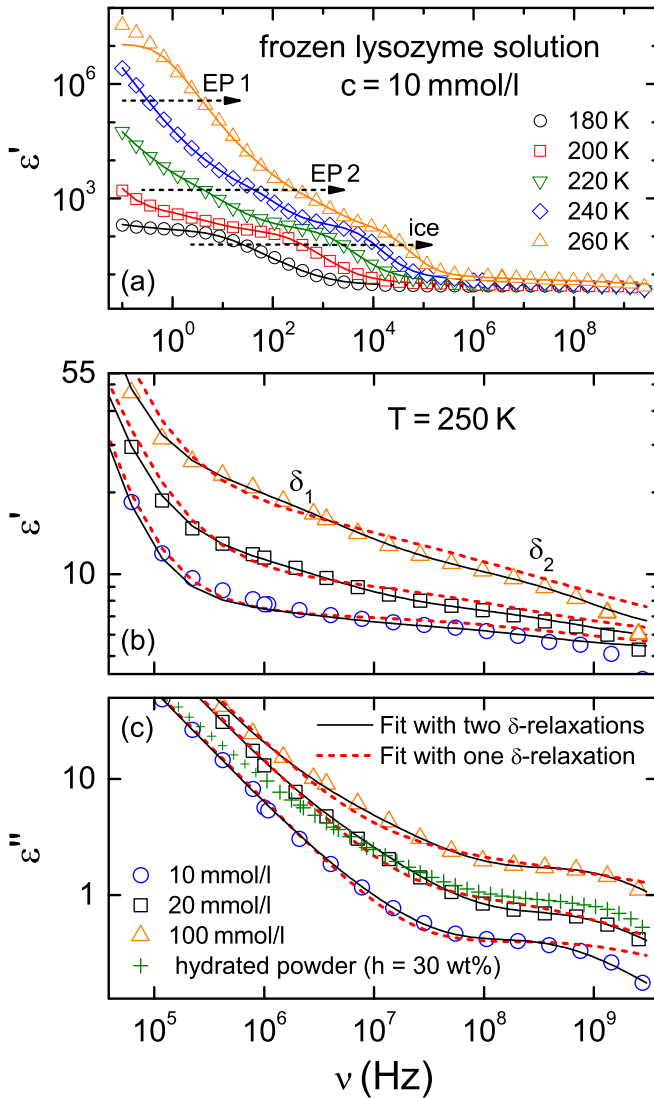


FIG. 2. (Color online) Dielectric spectra of frozen protein solutions. (a) Dielectric constant of a 10 mmol/l lysozyme solution measured at different temperatures below 273 K. The solid lines are fits using the sum of five Cole-Cole functions. (b),(c) Zoomed view of  $\epsilon'(\nu)$  (a) and  $\epsilon''(\nu)$  of differently concentrated protein solutions ( $c = 10, 20$ , and  $100$  mmol/l) measured at 250 K. Lines are fits using five (solid lines) or four (dashed lines) Cole-Cole functions in total. Pluses in (c) represent the dielectric loss of a hydrated lysozyme powder ( $h = 30$  wt%).

data of differently concentrated protein solutions measured at 250 K. Obviously, there is a relaxation process just below 1 GHz, revealed by a small step in  $\epsilon'$  (b) and a rather well-pronounced peak in  $\epsilon''$  (c). This relaxation,  $\delta_2$ , is clearly seen for all shown concentrations. For the highest concentrated sample, 100 mmol/l, faint indications for a second relaxation are found between  $10^6$  and  $10^7$  Hz. For the lower concentrated samples, this relaxation is less obvious but is clearly revealed by the fitting procedure described in the following.

The solid lines in Fig. 2 are fits using the sum of five Cole-Cole functions [50],  $\epsilon^*(\nu) = \sum_n \{\epsilon_\infty + \Delta\epsilon_n / [1 + (i\omega\tau_n)^{1-\alpha_n}]\}$ , to account for the five relaxations.

Here  $\tau$  and  $\Delta\epsilon$  represent the relaxation time and the dielectric strength, respectively. This function is an empirical extension of the Debye formula ( $\alpha = 0$ ) [51]; the additional parameter  $\alpha_n$  ( $0 \leq \alpha_n < 1$ ) causes a symmetric broadening of the relaxation peaks. For comparison, Figs. 2(b) and 2(c) also show fits with four Cole-Cole functions, i.e., using only one relaxation function to account for the  $\delta$ -dispersion range (dashed lines). In contrast to solutions above the freezing point [14], where the  $\beta$  and  $\gamma$  relaxations partly superimpose the  $\delta$ -dispersion region, obviously a satisfying description of the present frozen-solution data only is possible when assuming two  $\delta$  relaxations. This is a clear hint at the bimodality of the hydration-shell dynamics. As expected for hydration-water-related relaxations, the amplitudes of the  $\delta$  relaxations increase with increasing protein content, i.e., with increasing number of bound water molecules. The pluses in Fig. 2(c) represent  $\epsilon''(\nu)$  of a hydrated lysozyme powder sample with a hydration degree of  $h = 30$  wt%. The dielectric loss of this sample obviously resembles that of the 20 mmol/l solution. While the protein content of this sample is significantly higher than for the 20 mmol/l solution, the amount of water is clearly lower. Overall, this causes a  $\delta_2$  relaxation of similar dielectric strength. The properties of the  $\delta_1$  relaxation cannot be judged by eye, but are deduced and discussed below.

The most important parameter derived from the fits to the experimental data is the relaxation time  $\tau$ , characterizing the dynamics of the relaxing entities. In the case of thermally activated behavior, the temperature dependence of  $\tau$  can be described by the Arrhenius law,  $\tau = \tau_0 \exp[E_\tau / (k_B T)]$ , where  $\tau_0$  is the inverse attempt frequency (typically of the order of phonon frequencies) and  $E_\tau$  is the hindering barrier. In disordered matter, relaxation processes often show super-Arrhenius behavior, which can be described by the empirical VFT formula,  $\tau = \tau_0 \exp[DT_{VFT} / (T - T_{VFT})]$  [52,53]. Here  $D$  is the so-called strength parameter. Large or small  $D$  values imply small or strong deviations from thermally activated behavior, which is termed “strong” or “fragile” behavior, respectively [52,54].

The temperature dependence of the obtained relaxation times  $\tau_{\delta_1}$  and  $\tau_{\delta_2}$  of *frozen* protein solutions ( $c = 3$ – $100$  mmol/l), is shown in Fig. 3 (right of the vertical line marking the freezing point of water). In this Arrhenius presentation, a linear behavior reveals thermally activated behavior, whereas a curved temperature dependence is typical for fragile materials. This figure also includes the relaxation times of the  $\delta_1$  relaxation of 3 and 5 mmol/l lysozyme solutions *above* the freezing point, as published in [14] (left of dashed vertical line), literature values of the  $\delta$  relaxations as reported in [12,13,55] (different protein solutions), the relaxation times of pure water above the freezing point (own measurements) and of supercooled water from [56], as well as the relaxation times of the hydrated lysozyme powder with  $h = 30$  wt%. Obviously, the relaxation times  $\tau_{\delta_1}$ , derived from frozen protein solutions, nicely match those determined from solutions in the liquid state. The minor deviations (discontinuity around 273 K) for the  $\delta_1$  relaxation can be explained by the fact that the protein solutions above freezing point were fitted with only one  $\delta$  relaxation as explained above [14], whereas two relaxation functions were needed to describe the  $\delta$  dispersion in the case of the frozen protein solutions. This causes a slight

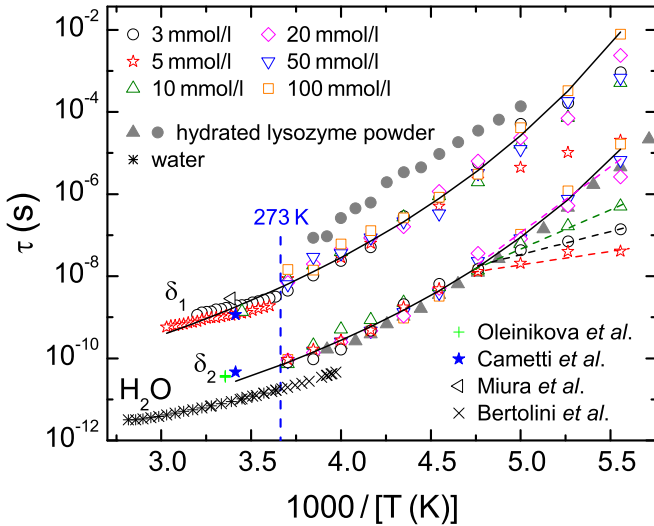


FIG. 3. (Color online) Relaxation times of the  $\delta_1$  and  $\delta_2$  relaxations of differently concentrated protein solutions ( $c = 3\text{--}100$  mmol/l) below the freezing point obtained in the present work. For comparison, literature data on  $\tau_{\delta_1}$  [13,14,55] and  $\tau_{\delta_2}$  [12,13] at  $T > 273$  K are included (Refs. [13,14,55]: lysozyme solutions; Ref. [12]: ribonuclease A). The full circles and triangles are the relaxation times of the two intrinsic relaxations found in a hydrated lysozyme powder [15] ( $h = 30$  wt%). The asterisks and crosses are the relaxation times of water (own data) and supercooled water [56], respectively. The lines are master curves using the VFT formula.

spectral shift of the  $\delta_1$  relaxation in the liquid solutions to higher frequencies, i.e., lower relaxation times. For the faster relaxation,  $\delta_2$ , the relaxation times of the frozen solutions are in very good accordance with the relaxation times reported for different protein solutions (ribonuclease A [12] and lysozyme [13]). The present results thus prove the proposed bimodality of the protein  $\delta$  dispersion.

Some researchers believe that both  $\delta$  relaxations are strongly correlated with the protein hydration shell [9,10,13]. However, for the slower relaxation ( $\delta_1$ ), protein-water collective motions or internal protein motions are alternative explanations [12,34,57]. Our own studies on hydrated proteins [15] show that this relaxation strongly depends on the degree of hydration. This is confirmed by the fact that the  $\delta_1$  relaxation of the hydrated powder ( $h = 30$  wt%) (full circles in Fig. 3) is significantly slower than the  $\delta_1$  relaxation of the fully hydrated protein solutions. As water is known to have a “lubricating” effect on proteins [57,58], it seems reasonable to ascribe this hydration-dependent relaxation to a correlated protein-water movement. In contrast, the  $\delta_2$  relaxation times of the hydrated protein powder (full triangles) agree with those of the frozen protein solutions. The dielectric strengths of the  $\delta_2$  relaxation of the protein powder and of the 20 mmol/l solutions are similar [cf. Fig. 2(c)]. This indicates that this relaxation not only depends on the amount of protein but also on the content of water in the sample. Moreover, it was found that this relaxation disappears when drying the protein powder [15]. These facts clearly suggest that the  $\delta_2$  relaxation arises from loosely bound hydration water.

To emphasize the fragile temperature characteristics of the relaxation times, VFT curves are drawn as solid lines in Fig. 3. For the  $\delta_1$  relaxation, the dynamics of nearly all samples follow this “master curve” ( $\tau_0 = 3.6 \times 10^{-13}$  s,  $D = 12.7$ ,  $T_{\text{VFT}} = 117.5$  K) throughout the whole temperature range. However, there are slight deviations from this behavior at the lowest temperatures investigated, especially for the 5 mmol/l solution. These deviations show no systematic development with concentration and can be explained by the fact that the determination of  $\tau_{\delta_1}$  tends to become increasingly difficult with decreasing temperature, i.e., its uncertainty increases.

The relaxation times of the  $\delta_2$  relaxation behave differently. At high temperatures, they follow a VFT master curve ( $\tau_0 = 2.4 \times 10^{-14}$  s,  $D = 10.3$ ,  $T_{\text{VFT}} = 119$  K), but at a temperature of approximately 210 K, the behavior of most samples changes to an Arrhenius temperature dependence, marked by the dashed lines. Interestingly, a very similar dynamic crossover was also found, e.g., by Chen *et al.* for fully hydrated lysozyme powder using neutron-scattering measurements [37] and for confined water [59–61]. However, as shown in Fig. 3 (closed triangles), our own dielectric measurements of the  $\delta_2$  relaxation in hydrated lysozyme powder with identical hydration level reveal no crossover behavior, a fact that remains to be explained. The crossover transition in frozen lysozyme solutions, observed in the present work, becomes less prominent with increasing protein concentration (Fig. 3), which might be explained by the fact that no complete hydration shell is formed for the samples with the highest protein concentrations (due to the lack of water) and thus the transition is suppressed. This is consistent with our results on the hydrated powder, where the water content is even lower.

The  $\delta_2$  relaxation is ascribed to the dynamics of loosely bound hydration water [9,12,13,57]. Thus it is tempting to speculate that the found dynamic crossover has some relation to the highly debated fragile-to-strong transition of bulk water [3,37,38,62–67], which is suspected to occur in the so-called No Man’s Land (about 160–235 K) afflicted by rapid crystallization. However, when assessing the possible relation of the found  $\tau_{\delta_2}(T)$  crossover to bulk-water dynamics, one should note that extrapolating the mentioned Arrhenius behavior of the  $\delta_2$  relaxation times at low protein concentrations to 100 s, leads to glass temperatures that are far below those suggested for bulk water [68,69]. Moreover, it also has to be stressed that the significance of the fragile-to-strong transition found in the present work is limited because  $\tau_{\delta_2}$  has high uncertainty, especially at low temperatures and concentrations (cf. Fig. 2) (see Appendix B for a further check of the significance of the transition).

#### IV. SUMMARY

In summary, the present study demonstrates the great value of dielectric measurements on frozen protein solutions, allowing one to circumvent various problems arising in investigations of liquid solutions or hydrated powders. With the help of these studies, the existence of a second  $\delta$  relaxation could be unequivocally proven. Moreover, comparing the results with measurements on lysozyme solutions

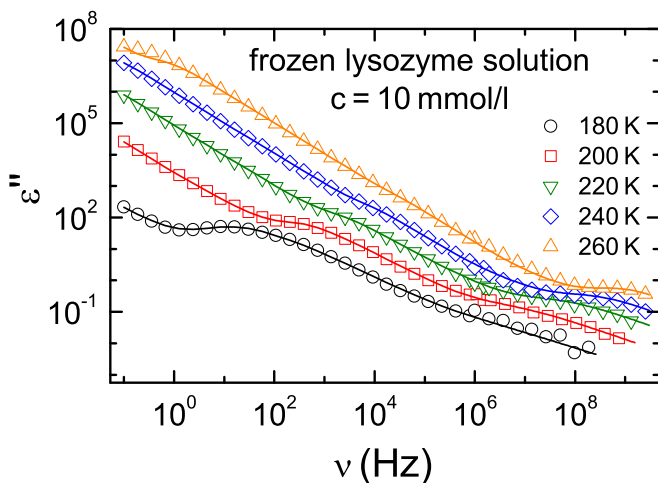


FIG. 4. (Color online) Dielectric loss of a 10 mmol/l lysozyme solution measured at different temperatures below 273 K. Solid lines are fits using the sum of five Cole-Cole functions.

above the freezing point and with hydrated powders enables a clear assignment of the  $\delta_2$  relaxation to loosely bound hydration water. For the  $\delta_1$  relaxation, due to its strong dependence on hydration, a collective protein-water motion seems most probable. In addition, indications for a transition from fragile to strong temperature characteristics of the  $\delta_2$  relaxation were found at low temperatures. This dynamic change turned out to depend on the protein concentration of the solutions, becoming less prominent for high protein concentrations. Further studies in frozen solutions of different proteins and with higher resolution are necessary to help solve the origin and significance of this fragile-to-strong transition.

#### APPENDIX A: BROADBAND DIELECTRIC LOSS SPECTRA

Figure 4 shows the frequency dependence of the dielectric loss  $\varepsilon''(\nu)$  of the 10 mmol/l lysozyme solution measured at the same temperatures as  $\varepsilon'(\nu)$  shown in Fig. 2(a). As mentioned in Sec. III, there are three relaxations besides the two  $\delta$  relaxations. Except for the strongest relaxation (EP1), the corresponding relaxation peaks of the dielectric loss are superimposed by the strong dc conductivity contributing to the loss according to  $\varepsilon''(\nu) = \sigma' / (\varepsilon_0 2\pi\nu)$ , which gives rise to a  $1/\nu$  divergence in  $\varepsilon''(\nu)$  for decreasing frequencies. With decreasing temperature, the ice relaxation emerges and can clearly be seen for the lowest temperature shown (180 K). The solid lines are fits using the sum of five Cole-Cole functions to account for the five relaxations found.

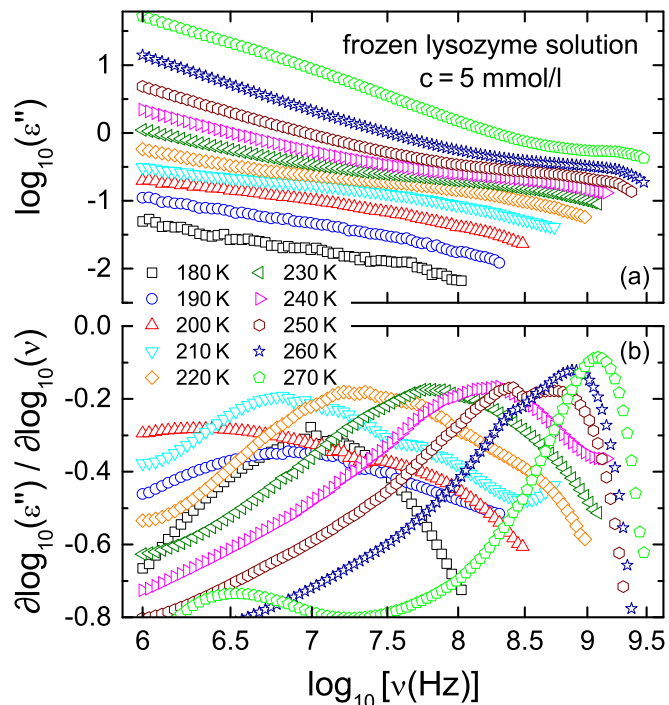


FIG. 5. (Color online) (a) Frequency dependence of the dielectric loss of the 5 mmol/l lysozyme solution for temperatures below the freezing point. (b) First derivative  $\partial \log_{10}(\varepsilon'') / \partial \log_{10}(\nu)$  of the data shown in (a). To avoid excessive scattering, before calculating the derivatives, the data in (a) were smoothed by Savitzky-Golay filtering using 5th-order polynomials.

#### APPENDIX B: SIGNIFICANCE OF THE FRAGILE-TO-STONG TRANSITION

Figure 5(a) shows the high-frequency part of the dielectric loss  $\varepsilon''(\nu)$  of the 5 mmol/l lysozyme solution and Fig. 5(b) shows the derivative  $\partial \log_{10}(\varepsilon'') / \partial \log_{10}(\nu)$  (=slope), in the temperature range 180–270 K. As mentioned in Sec. III, the significance of the fragile-to-strong transition found for the temperature dependence of the relaxation times at around 210 K is limited. This is because the exact loss-peak positions are difficult to determine for the low-temperature curves [see Fig. 5(a)]. Therefore, the slope of the curves was determined by calculating the first derivative of the dielectric loss [Fig. 5(b)]. The maxima in Fig. 5(b) correspond to the points with the most shallow slope in the experimental data, indicating a step in  $\varepsilon''(\nu)$  caused by an underlying relaxation peak. In this way, the temperature dependence of the  $\delta_2$  relaxation can be tracked. Starting at 270 K, the peak strongly shifts with decreasing temperature but then gets stuck somewhere below 210 K. This finding seems to support the fragile-to-strong transition of the relaxation times (Fig. 3).

- [1] R. Gregory, in *Protein-Solvent Interactions*, edited by R. Gregory (Marcell Dekker, New York, 1994).  
 [2] I. D. Kuntz and W. Kauzmann, *Adv. Protein Chem.* **28**, 239 (1974).

- [3] W. Doster, S. Busch, A. M. Gaspar, M. S. Appavou, J. Wuttke, and H. Scheer, *Phys. Rev. Lett.* **104**, 098101 (2010).  
 [4] C. Cametti, S. Marchetti, and G. Onori, *J. Phys. Chem. B* **117**, 104 (2013).

- [5] K. L. Ngai, S. Capaccioli, S. Ancherbak, and N. Shinyashiki, *Philos. Mag.* **91**, 1809 (2011).
- [6] K. L. Ngai, S. Capaccioli, and A. Paciaroni, *Chem. Phys.* **424**, 37 (2013).
- [7] V. C. Nibali and M. Havenith, *J. Am. Chem. Soc.* **136**, 12800 (2014).
- [8] B. H. McMahon, H. Frauenfelder, and P. W. Fenimore, *Eur. Phys. J. Spec. Top.* **223**, 915 (2014).
- [9] E. H. Grant, V. E. R. McClean, N. R. V. Nightingale, R. J. Sheppard, and M. J. Chapman, *Bioelectromagnetics* **7**, 151 (1986).
- [10] S. Bone and Z. Bogumil, *Bioelectronics* (Wiley, New York, 1992).
- [11] A. Knocks and H. Weingärtner, *J. Phys. Chem. B* **105**, 3635 (2001).
- [12] A. Oleinikova, P. Sasisanker, and H. Weingärtner, *J. Phys. Chem. B* **108**, 8467 (2004).
- [13] C. Cametti, S. Marchetti, C. M. C. Gambi, and G. Onori, *J. Phys. Chem. B* **115**, 7144 (2011).
- [14] M. Wolf, R. Gulich, P. Lunkenheimer, and A. Loidl, *Biochim. Biophys. Acta* **1824**, 723 (2012).
- [15] M. Wolf, *The Dynamics of Proteins, Water and their Interactions – A Dielectric Study* (Verlag Dr. Hut, Munich, 2014).
- [16] J. R. Macdonald, *Impedance Spectroscopy – Emphasizing Solid Materials and Systems* (Wiley, New York, 1987).
- [17] Y. Feldman, I. Ermolina, and Y. Hayashi, *IEEE Trans. Dielectr. Electr. Insul.* **10**, 728 (2003).
- [18] A. Pimenov, J. Ullrich, P. Lunkenheimer, A. Loidl, and C. H. Rüscher, *Solid State Ionics* **109**, 111 (1998).
- [19] R. Gulich, M. Köhler, P. Lunkenheimer, and A. Loidl, *Radiat. Environ. Biophys.* **48**, 107 (2009).
- [20] S. Emmert, M. Wolf, R. Gulich, S. Krohns, S. Kastner, P. Lunkenheimer, and A. Loidl, *Eur. Phys. J. B* **83**, 157 (2011).
- [21] M. Wolf, R. Gulich, P. Lunkenheimer, and A. Loidl, *Biochim. Biophys. Acta* **1810**, 727 (2011).
- [22] F. Perrin, *J. Phys. Radium* **5**, 497 (1934).
- [23] S. H. Koenig, *Biopolymers* **14**, 2421 (1975).
- [24] C. G. Essex, M. S. Symonds, R. J. Sheppard, E. H. Grant, R. Lamote, F. Soetewey, M. Y. Rosseneu, and H. Peeters, *Phys. Med. Biol.* **22**, 1160 (1977).
- [25] V. D. Fedotov, Y. D. Feldman, A. G. Krushelnitsky, and I. V. Ermolina, *J. Mol. Struct.* **219**, 293 (1990).
- [26] I. V. Ermolina, V. D. Fedotov, and Y. D. Feldman, *Physica A* **249**, 347 (1998).
- [27] G. P. Johari and M. Goldstein, *J. Chem. Phys.* **53**, 2372 (1970).
- [28] A. Kudlik, S. Benkhof, T. Blochowicz, C. Tschirwitz, and E. Roessler, *J. Mol. Struct.* **479**, 201 (1999).
- [29] S. Kastner, M. Kohler, Y. Goncharov, P. Lunkenheimer, and A. Loidl, *J. Non-Cryst. Solids* **357**, 510 (2011).
- [30] J. Swenson and S. Cervený, *J. Phys.: Condens. Matter* **27**, 033102 (2015).
- [31] G. P. South and E. H. Grant, *Proc. R. Soc. London, Ser. A* **328**, 371 (1972).
- [32] D. Ban, M. Funk, R. Gulich, D. Egger, T. M. Sabo, K. F. A. Walter, R. B. Fenwick, K. Giller, F. Pichierri, B. L. de Groot, O. F. Lange, H. Grubmueller, X. Salvatella, M. Wolf, A. Loidl, R. Kree, S. Becker, N.-A. Lakomek, D. Lee, P. Lunkenheimer, and C. Griesinger, *Angew. Chem. Int. Ed.* **50**, 11437 (2011).
- [33] S. Bone, *Biochim. Biophys. Acta* **916**, 128 (1987).
- [34] E. H. Grant, R. J. Sheppard, and G. P. South, *Dielectric Behaviour of Biological Molecules in Solution* (Clarendon, Oxford, 1978).
- [35] B. E. Pennock and H. P. Schwan, *J. Phys. Chem.* **73**, 2600 (1969).
- [36] W. Doster, S. Cusack, and W. Petry, *Nature* **337**, 754 (1989).
- [37] S. H. Chen, L. Liu, E. Fratini, P. Baglioni, A. Faraone, and E. Mamontov, *Proc. Natl. Acad. Sci. USA* **103**, 9012 (2006).
- [38] S. Khodadadi, S. Pawlus, J. H. Roh, V. G. Sakai, E. Mamontov, and A. P. Sokolov, *J. Chem. Phys.* **128**, 195106 (2008).
- [39] E. Tombari and G. P. Johari, *J. Chem. Phys.* **139**, 105102 (2013).
- [40] S. Khodadadi, S. Pawlus, and A. P. Sokolov, *J. Phys. Chem. B* **112**, 14273 (2008).
- [41] F. Pizzitutti and F. Bruni, *Phys. Rev. E* **64**, 052905 (2001).
- [42] R. Pethig, *Ann. Rev. Phys. Chem.* **43**, 177 (1992).
- [43] J. A. Rupley and G. Careri, *Adv. Protein Chem.* **41**, 37 (1991).
- [44] G. P. Johari and E. Whalley, *J. Chem. Phys.* **75**, 1333 (1981).
- [45] V. F. Petrenko and W. R. Whitworth, *Physics of Ice* (Oxford University Press, Oxford, 2006).
- [46] R. Böhmer, M. Maglione, P. Lunkenheimer, and A. Loidl, *J. Appl. Phys.* **65**, 901 (1989).
- [47] U. Schneider, P. Lunkenheimer, A. Pimenov, R. Brand, and A. Loidl, *Ferroelectrics* **249**, 89 (2001).
- [48] S. R. Gough and D. W. Davidson, *J. Chem. Phys.* **52**, 5442 (1970).
- [49] N. Shinyashiki, W. Yamamoto, A. Yokoyama, T. Yoshinari, S. Yagihara, R. Kita, K. L. Ngai, and S. Capaccioli, *J. Phys. Chem. B* **113**, 14448 (2009).
- [50] K. S. Cole and R. H. Cole, *J. Chem. Phys.* **9**, 341 (1941).
- [51] P. Debye, *Polar Molecules* (Dover, New York, 1929).
- [52] C. A. Angell, in *Relaxations in Complex Systems*, edited by K. L. Ngai and G. B. Wright (Springer, New York, 1985).
- [53] C. A. Angell, *J. Non-Cryst. Solids* **102**, 205 (1988).
- [54] R. Böhmer, K. L. Ngai, C. A. Angell, and D. J. Plazek, *J. Chem. Phys.* **99**, 4201 (1993).
- [55] N. Miura, N. Asaka, N. Shinyashiki, and S. Mashimo, *Biopolymers* **34**, 357 (1994).
- [56] D. Bertolini, M. Cassettari, and G. Salvetti, *J. Chem. Phys.* **76**, 3285 (1982).
- [57] S. Bone and R. Pethig, *J. Mol. Biol.* **157**, 571 (1982).
- [58] R. Pethig, in *Protein-Solvent Interactions*, edited by R. Gregory (Marcell-Dekker, New York, 1994).
- [59] F. Ridi, P. Luciani, E. Fratini, and P. Baglioni, *J. Phys. Chem. B* **113**, 3080 (2009).
- [60] L. Liu, S. H. Chen, A. Faraone, C. W. Yen, C. Y. Mou, A. I. Kolesnikov, E. Mamontov, and J. Leao, *J. Phys.: Condens. Matter* **18**, S2261 (2006).
- [61] J. M. Zanotti, M. C. Bellissent-Funel, and S. H. Chen, *Europhys. Lett.* **71**, 91 (2005).
- [62] K. Ito, C. T. Moynihan, and C. A. Angell, *Nature* **398**, 492 (1999).
- [63] G. P. Johari, *Phys. Chem. Chem. Phys.* **2**, 1567 (2000).
- [64] P. G. Debenedetti, *J. Phys.: Condens. Matter* **15**, R1669 (2003).
- [65] C. A. Angell, *Science* **319**, 582 (2008).
- [66] M. Vogel, *Phys. Rev. Lett.* **101**, 225701 (2008).
- [67] M. Nakanishi, P. Griffin, E. Mamontov, and A. P. Sokolov, *J. Chem. Phys.* **136**, 124512 (2012).
- [68] G. P. Johari, A. Hallbrucker, and E. Mayer, *Nature* **330**, 552 (1987).
- [69] Y. Z. Yue and C. A. Angell, *Nature* **427**, 717 (2004).